mass spectrometric and gas chromatographic analyses have indicated that CO and CO_2 account for over 95% of the total volatiles. CO production, in most cases, was reported to be 2–4 times as great as CO_2 production and was dependent upon the duration of UV exposure. Thermal decomposition on the other hand yielded CO_2 as the major volatile product. The minor amount of carbon dioxide detected following plasma initiation here also supports the Norrish type I decomposition pathway.

Two mechanisms, dependent on the degree of treatment severity, are therefore most probable. Initially, at low energy input a relaxation process that forms a new carbonyl structure (Norrish type I ester cleavage) is favored. If the energy is higher, then loss of carbon monoxide is favored. The adhesive strength of metalized PET follows this trend in behavior. That is, at low plasma exposure the production of active surface species may provide reaction sites between the polymer and the metal that allows increased adhesion. High plasma exposure leads to substantial chain scission and loss of CO before metalization. A weak boundary layer, consisting of low molecular weight polymer, may be formed by this degradation and thereby decrease adhesion. The small amount of CO_2 detected suggests that chain scission between the ester oxygen and the primary methylene group is minor (Norrish type II). Further details regarding the adhesion mechanism of titanium to these plasma-treated PET films will be reported in a subsequent paper.

(21) Wiles, D. M. *Degradation and Stabilization of Polymers*; Wiley: New York, 1975; p 137.

Registry No. PET, 25038-59-9; N_2O, 10024-97-2; Ar, 7440-37-1.

Molecular- and Atomic-Beam Scattering from Surfaces. Dynamics of Gas–Surface Interactions and Mechanisms of Condensation of Cesium Iodide Molecules and Cesium Atoms Incident on NaCl(c,100)

T. Brown, M. Kliewer, K. Pranata, E. Heyman, and R. Schoonmaker*

Department of Chemistry, Oberlin College, Oberlin, Ohio 44074

Received August 20, 1990. Revised Manuscript Received November 19, 1990

Mechanisms of condensation are given for molecular beams of CsI(g) and Cs(g) that are incident on clean and beam-deposited NaCl(c,100) surfaces, and dynamics of gas–surface interactions for these systems are discussed. Reflection coefficients and angular distributions of scattered molecules have been determined at several angles from normal to near glancing incidence of the molecular beams and as a function of equivalent monolayer coverage of the surface by molecules deposited from the molecular beam. Intensities of molecules scattered at the specular angle have been measured as a function of equivalent monolayer coverage of the surface.

Introduction

Most chemical and physical processes occur at interfaces. For example, interactions of gas molecules with a surface play a crucial role in processes as diverse as heterogeneous catalysis, corrosion, lift and drag on vehicles in flight, atmospheric precipitation and fabrication of integrated circuits. In materials science, development of new processing strategies to support high technology requires knowledge about microscopic mechanisms of growth and removal of atoms or molecules from surfaces of metals, semiconductors, insulators, polymers, ceramics, and composites.[1] In recent years a great deal of effort, both theoretical and experimental, has been expended and corresponding progress made in understanding processes which occur at the gas–metal and gas–semiconductor interfaces; but there has been much less activity associated with investigation of the gas–insulator interface, which has been the subject of continuing study in this laboratory. The present work continues our series of investigations[2-5] of gas–surface interactions and condensation of gaseous alkali metal halide molecules on alkali metal halide crystal surfaces and extends it to include interaction of alkali metal atoms with alkali metal halide surfaces.

Condensation of a gas on a solid surface may be characterized by complex combinations of kinetic processes that always involve a collision at the surface that may be accompanied or followed by thermal and momentum accommodation, adsorption, surface diffusion, nucleation, reevaporation, etc. The condensation coefficient, α_C, is defined as the fraction of gas molecules striking a surface that condenses. The reflection coefficient, $\alpha_R = (1 - \alpha_C)$, is the fraction of incident molecules that is restituted to the gas phase after collision with the surface. There is a close connection between the dynamics of the gas–surface collision and the condensation (or reflection) coefficient and between α_C (or α_R) and the mechanism of condensation. At the present time it is not possible by either classical or quantum methods to make a reliable a priori calculation of the coefficient for condensation of any gas on any surface or to predict from theory the detailed mechanism and rate-controlling steps in the condensation of molecules on surfaces. In the absence of an exact, detailed and computationally tractable method for treating the dynamics of gas–surface collisions and the mechanism of condensation, our experimental program has been established to measure coefficients for condensation of gas

(1) Chaudhari, P. *Phys. Today* **1984**, *37*, 160.
(2) Schoonmaker, R.; Lo, V. *J. Chem. Phys.* **1973**, *58*, 727.
(3) Schoonmaker, R.; Tu, L. *J. Chem. Phys.* **1974**, *60*, 4650.
(4) O'Connor, P.; Schoonmaker, R. *J. Phys. Chem.* **1976**, *80*, 390.
(5) Baker, S.; Schoonmaker, R. *J. Appl. Phys.* **1985**, *58*, 2091.

0897-4756/91/2803-0298$02.50/0

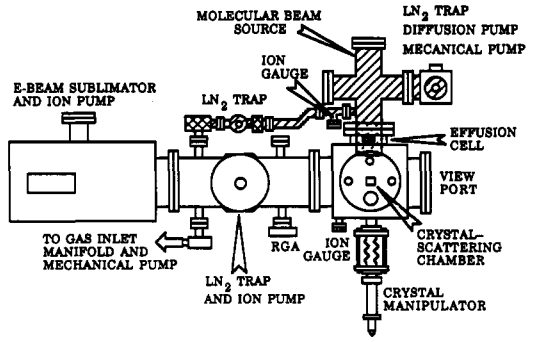

Figure 1. Schematic diagram of the molecular beam apparatus.

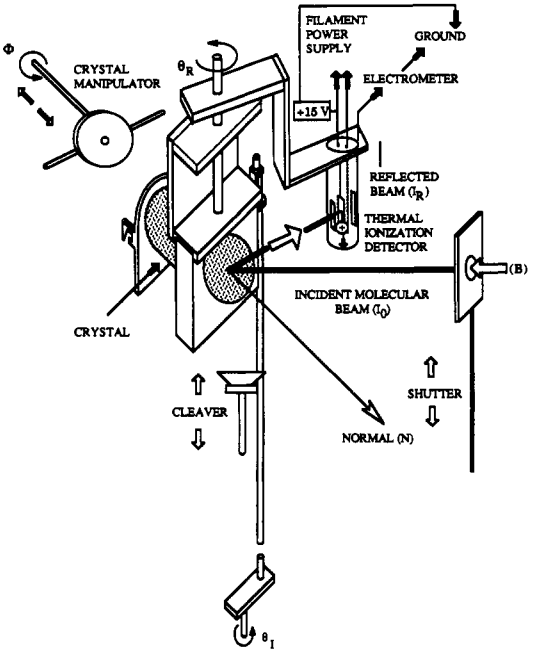

Figure 2. Internal parts of the scattering chamber.

molecules on solid surfaces and to study the dynamics of gas–surface interactions with the purpose of elucidating mechanisms of condensation.

The work reported here involves CsI(g) and Cs(g) interactions with clean and beam-deposited NaCl(c,100) surfaces. Previously reported results[5] for scattering of molecular beams of RbI(g) from NaCl(c,100) are analogous to results reported in the present work for CsI(g)/NaCl(c,100) although different behavior has been observed in our investigations of other [alkali metal halide(g)/NaCl(c,100)] systems.[6]

Experimental Section

In our method, a well-collimated effusive beam of molecules, with a Maxwell–Boltzmann distribution of energy, is directed at a surface where some of the molecules condense and others are scattered back to the gas. Because the intensity and angular distribution of scattered molecules depend on the nature of the surface, the molecular beam is itself a sensitive probe that allows us to investigate the fate of what goes on to the surface by making measurements on what comes off.

The molecular beam scattering apparatus, Figure 1, is similar to one that has been previously described[5] except that there is a new scattering chamber and UHV pumping system that has a base pressure of $\sim 2 \times 10^{-11}$ Torr. Figure 2 shows internal parts of the scattering chamber including the thermal ionization detector for molecules incident on the surface of the crystal and scattered from it. It should be emphasized that ionization of alkali metal atoms that are incident on the hot rhenium filament of the detector provides a direct measure of *flux* for the atomic beam that is incident on, or scattered from, a surface; hence, it is possible to calibrate the rate at which Cs atoms arrive at the surface of the crystal from our effusion source where the atomic beam is produced by a solid-state reaction of powdered cesium chromate (99.9%, Atomergic Chemicals) with finely powdered silicon metal.[7] The CsI molecular beam is generated by effusion from a molybdenum cell containing CsI (c, ultrapure, Alfa Products, Ventron). 100-oriented single-crystals of NaCl (Harshaw Chemical Co.), similar to those described by Schoonmaker and Lo,[2] are 25 mm in diameter and 50 mm long. The molecular beam path and scattering geometry, which is used in displaying angular distributions in the results section, are shown in Figure 3. The molecular or atomic beam diameter at the point of impact with the surface of the crystal is ~2 mm. The detector has an angular resolution of slightly less than 1°. The experimental procedure has been discussed in detail[5] previously and is only outlined here: (1) with the scattering chamber at $\sim(1\text{–}5) \times 10^{-10}$ Torr and the effusion source at a temperature that produces a stable beam of desired flux, the shutter plate is opened and the intensity, I_0, of the molecular beam is measured; (2) the shutter plate is closed and the 100–oriented single-crystal of NaCl is cleaved in situ to produce a clean, well-defined surface; (3) the shutter plate is opened to expose the surface to the molecular beam; (4) for a selected angle of incidence, θ_I, a complete angular distribution is determined by measuring the intensity of the scattered molecular beam, I_R, as a function of scattering angle from edge to edge of the crystal, $-90° \leq \theta_R \leq +90°$, Figure 3b; or for selected angles of incidence and reflection, the intensity of the scattered molecular beam is measured as a function of time, i.e., as a function of equivalent monolayers, EML, of the molecular beam material deposited on the surface. Molecular beam flux and temperatures

Table I. Experimental Conditions and Reflection Coefficients for Molecular Beams of CsI Scattered from NaCl(c,100)

run[a]	θ_I[b]/deg	α_R[c]/10^{-4}	run[a]	θ_I[b]/deg	α_R[c]/10^{-4}
TB-12	0	1.2[d]	TB-9	45	1.2
TB-22	0	1.3[d]	TB-15	45	1.4
TB-7	30	0.94	TB-18	45	1.4
TB-8	30	1.3	TB-11	60	1.2
TB-14	30	1.4	TB-16	60	1.1
TB-19	30	1.2	TB-21	60	1.3
TB-29	30	0.96	TB-30	70	0.82

[a] $T_{surface}$, 318 ± 2 K; T_{beam}, 723 ± 1 K; molecular beam flux, (2.7 ± 0.2) × 10^{11} molecules cm^{-2} s^{-1}; Φ, 0°C. [b] Angle of incidence. [c] Reflection coefficient; fraction of incident gas molecules that is restituted to the gas phase after collision with the surface. All surfaces are clean, UHV-cleaved NaCl(c,100). [d] $\alpha_R = 7.2 \times 10^{-4}$ if it is assumed that, owing to symmetry in the case of normal incidence, out-of-plane scattering has a cosine component that is identical to the in-plane cosine component.

Table II. Experimental Conditions and Reflection Coefficients for Atomic Beams of Cs Scattered from NaCl(c,100)

run[a]	θ_I[b]/deg	α_R[c]
EH-21	0	0.20[d]
EH-22	30	0.16
EH-16	45	0.19
EH-14[e]	45	0.21
EH-23	60	0.21
EH-24	75	0.11

[a] $T_{surface}$, 311 ± 2 K; T_{beam}, 679 ± 1 K; atomic beam flux (0.96 ± 0.14) × 10^{11} atoms cm^{-2} s^{-1}; Φ, 0°. [b] Angle of incidence. [c] Reflection coefficient; fraction of incident gas molecules restituted to the gas phase after collision with the surface. Surfaces are UHV-cleaved NaCl(c,100) and clean, except where otherwise noted in *e*. [d] Lower limit, not all out-of-plane scattering is intercepted by the detector. [e] 1.7 EML of Cs previously deposited on the surface.

(6) Schoonmaker, R.; Grant, M.; Kliewer, M. Unpublished angular distributions for the systems CsF(g)/NaCl(c,100) and NaCl(g)/NaCl(c,100).

(7) Liu, M.; Wahlbeck, P. *J. Phys. Chem.* **1976**, *80*, 1484.

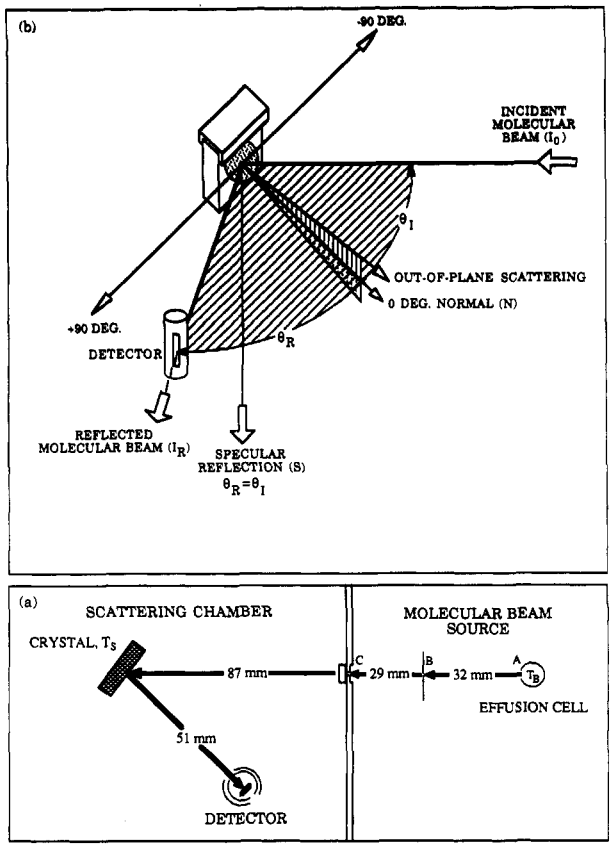

Figure 3. (a) Molecular beam path; A, orifice, 1.08-mm diameter; B, slit, 0.080 mm wide; C, orifice, 1.58-mm diameter; (b) scattering geometry.

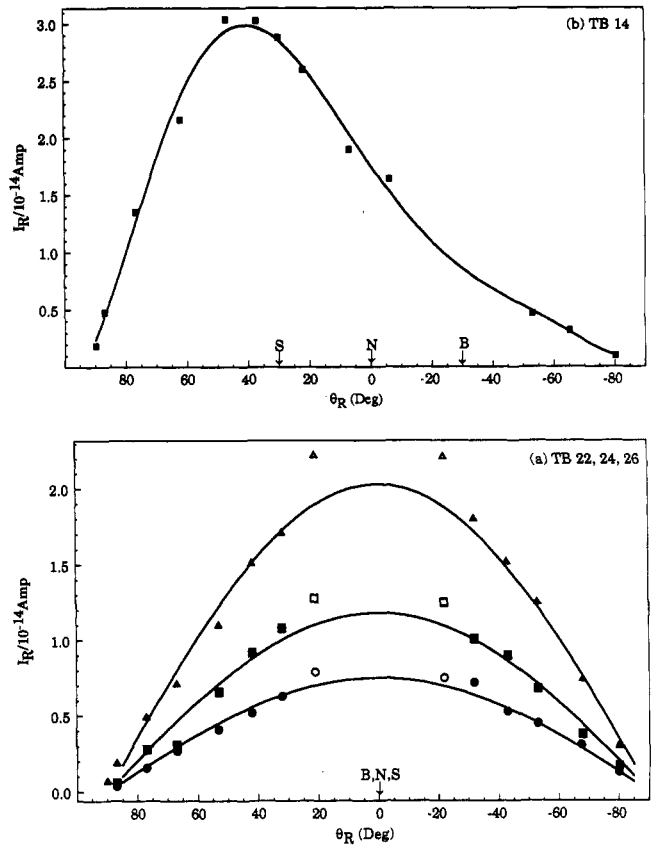

Figure 4. Angular distributions of CsI molecules scattered from NaCl(c,100). (a) $\theta_I = 0°$; triangles, clean surface (0.0–0.14 EML CsI deposited); squares, 0.38–0.52 EML; circles, 0.55–0.68 EML; solid line is best cosine (diffuse component of scattering) fit to data; open symbols, direct-inelastic component of scattering; region between open symbols on either side of normal is obscured by the width of the detector. (b) $\theta_I = 30°$; clean surface.

of the molecular beam and surface are listed in Tables I and II for all runs in which angular distributions are shown (Figures 4–6, 8–10). The total time from cleaving the crystal to completion of an angular distribution is ~20 min, during which the shutter is open and the crystal is exposed to the molecular beam for ~2 min or less. Thus, at UHV, contamination of the cleaved, clean crystal surface by residual gas is negligible and with the low beam flux used in these experiments less than 0.15 equivalent monolayer of beam material strikes the surface while an angular distribution is being measured.

The reflection coefficient, α_R, is determined as the ratio of intensity of scattered molecules, integrated over their angular distribution, to the intensity of incident molecules, integrated over the molecular beam profile.

Results and Discussion

The term "equivalent monolayer" (EML) is used to denote the fraction of a monolayer, or number of multiple monolayers, of CsI or Cs that *would have been* deposited on the originally clean NaCl surface *if* all molecules or atoms in the incident beam condensed by formation of successive, uniformly packed, two-dimensional layers. Along the abscissas of all the angular distributions that are presented, B designates the angle of incidence of the molecular or atomic beam on the surface, N the position of the normal to the surface, and S the position of specular reflection. Results for the dynamical interaction and mechanism of condensation of Cs(g) with NaCl(c,100) are best discussed in relation to those for CsI(g)/NaCl(c,100) with which we begin.

A. CsI(g)/NaCl(c,100). Angular distributions of CsI molecules scattered from clean and beam-deposited NaCl(c,100) surfaces at angles from normal to near glancing incidence are shown in Figures 4–6. Experimental conditions and measured reflection coefficients, α_R, for the runs shown in the figures are given in Table I. The results for runs with molecular beams of CsI are similar to those previously reported[5] for corresponding runs with molecular beams of RbI. For molecular beams of either CsI, Figure 4a, or RbI striking the surface at normal incidence, where incoming gas molecules have momentum only perpendicular to the surface, the angular distributions of reflected molecules have a large cosine component owing to randomization of perpendicular and parallel components of momentum during collisional interaction with the surface. Thus, during head-on collisions with smaller, lighter elements of an NaCl surface, the massive CsI or RbI projectiles must penetrate deeply into the repulsive part of the gas–surface potential and undergo battering from multiple perpendicular and parallel collisions, owing to surface vibrations of sodium and chloride ions, before exiting and being restored to the free gas state. It should also be noted that with both CsI, Figure 4a, and RbI beams at normal incidence, there is a definite, but mostly obscured, direct-inelastic component of the angular distribution of scattered molecules. For both CsI and RbI beams with angles of incidence on clean NaCl(c,100) of 30°, 45°, 60°, and 70°, angular distributions of scattered molecules are all concave up in the backscattering region, $0° \leq \theta_R \leq -90°$, Figures 4b, 5, and 6, which implies the absence of a cosine component; hence, for $\theta_I \geq 30°$, there is neither equilibration nor randomization of perpendicular and parallel components of momentum during collisional interaction with the surface. The difference in behavior at normal and nonnormal incidence probably is a consequence of the relatively smaller penetration of the repulsive wall of the gas–surface potential during collisions with θ_I

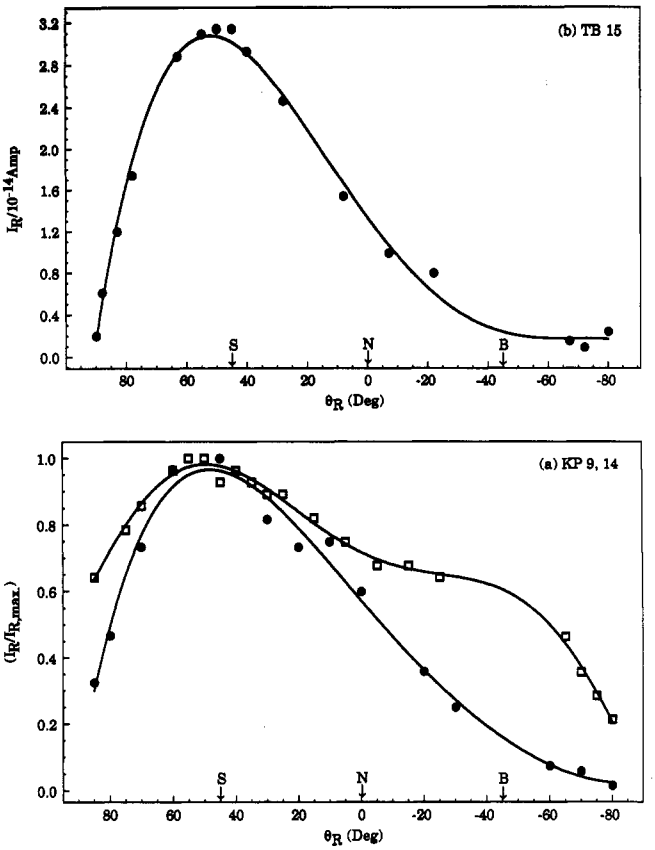

Figure 5. Angular distributions of CsI molecules scattered from NaCl(c,100). (a) $\theta_I = 45°$: normalized to $I_{R,max}$, circles, clean NaCl(c,100); squares, surface heavily beam-deposited (~20 EML CsI). (b) $\theta_I = 45°$, clean surface.

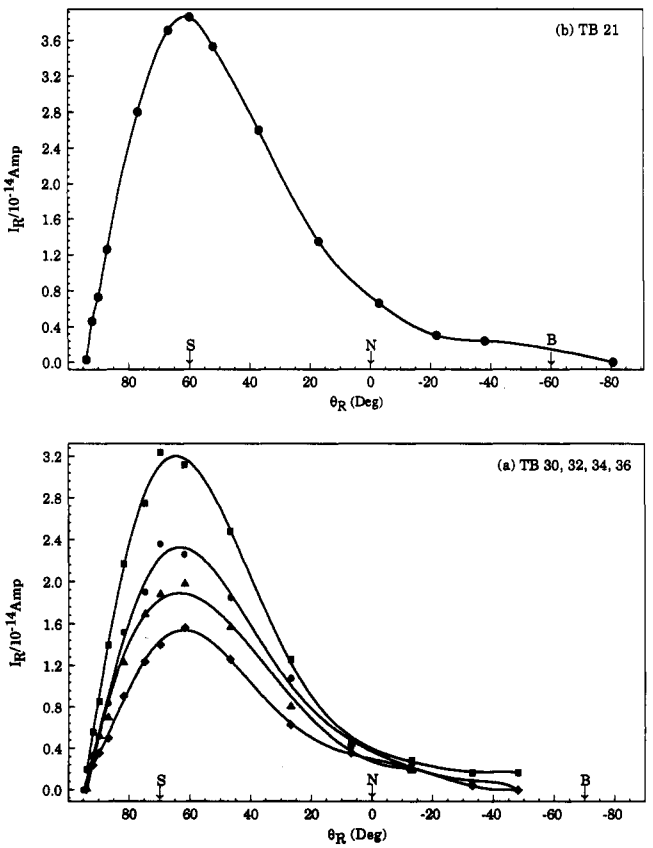

Figure 6. Angular distributions of CsI molecules scattered from NaCl(c,100) surfaces. (a) $\theta_I = 70°$; squares, clean surface, 0.0–0.06 EML CsI; circles, 0.11–0.18 EML; triangles, 0.25–0.31 EML; diamonds, 0.38–0.49 EML. (b) $\theta_I = 60°$, clean surface.

$\geq 30°$ owing to considerably smaller translational energy, $E_\perp = E_{trans} \cos^2 \theta_I$, and momentum of the incident particle in the direction normal to the surface. When a CsI beam impinges on an NaCl surface that has been heavily deposited (~20 EML) with CsI, Figure 5a, a large diffuse component, associated with random scattering by elements of a roughened surface, in the angular distribution of scattered molecules is readily apparent in the pronounced downward concavity of the backscattering region.

In the interest of brevity and because the results for CsI and RbI molecular beams incident on clean and beam-covered NaCl(c,100) are essentially identical, we shall summarize features of dynamics of the gas–surface interaction and the mechanism of condensation for the CsI(g)/NaCl(c,100) system and sketch in some supporting explanation. Detailed argument is available elsewhere.[5]

1. Dynamics of the gas–surface interaction for CsI(g)/NaCl(c,100): (a) Scattering follows classical mechanics ($\lambda_{deBroglie\ CsI(g)} \ll d_{NaCl(c,100)}$): no diffraction, no rainbows (Figures 4–6). (b) Scattering is independent of azimuthal angle, Φ. (c) Most incident CsI(g) molecules condense on a clean NaCl(c,100) surface, $\alpha_R \sim 10^{-4}$, Table I. A lower temperature molecular beam of CsI that effuses from a cell that is aligned with collimating slits has a larger reflection coefficient than a higher temperature CsI beam that effuses from a misaligned cell giving similar flux at the surface. Thus, we infer that it is not primarily molecules in the high-energy tail of the Maxwell–Boltzmann translational energy distribution that are reflected on collision with the surface. Reflected molecules may be those with unfavorable rotational orientation and impact parameter at collision with the surface.[5] (d) Angular distributions of scattered CsI molecules are much broader (fwhm) than the directed component of scattered Cs atoms, Figures 5b and 9a. The large breadth (fwhm), Figures 4–6, of angular distributions of scattered molecules results primarily from translational energy ⇒ rotational energy transfer for gas molecules during collision with the surface.[5] (e) For $\theta_I > 0°$, angular distributions are concave up in the backscattering region, Figures 4b, 5b, and 6, indicating the absence of a cosine or diffuse scattering component. Thus, reflected (scattered) molecules have had a very short lifetime of no more than a few vibrations[5] on the surface because they have not had perpendicular and parallel components of momentum randomized prior to restitution to the gas. (f) For CsI(g) molecules, the larger component (perpendicular or parallel) of momentum is preferentially transferred to the surface during the gas–surface collision,[5] Figures 4b, 5, and 6. (g) For CsI(g) striking clean NaCl(c,100), the fraction of gas molecules that condenses is independent of the angle of incidence in the range θ_I = 30–60° but increases near glancing incidence, Table I, presumably, because near glancing incidence (1) the perpendicular component of translational energy and momentum of the gas molecule becomes small and (2) the probability of the gas molecule hopping along the surface and undergoing multiple collisions increases. Both 1 and 2 should enhance trapping probability. (h) The fraction of incident gas molecules that condenses for [CsI(g)/CsI(c)] is larger than the fraction for [CsI(g)/NaCl(c,100)], Figure 7a, because in the former there is a softer surface, [θ_{Debye}(CsI) ≪ θ_{Debye}(NaCl)], and a much better mass match between gas and surface resulting in more effective gas ⇒ surface energy and momentum transfer.[5] Moreover, the binding energy of CsI that is adsorbed on CsI(c) is larger than the binding energy for CsI(ads) on NaCl(c,100) owing to much better registry between adsorbed CsI and the CsI substrate.[8]

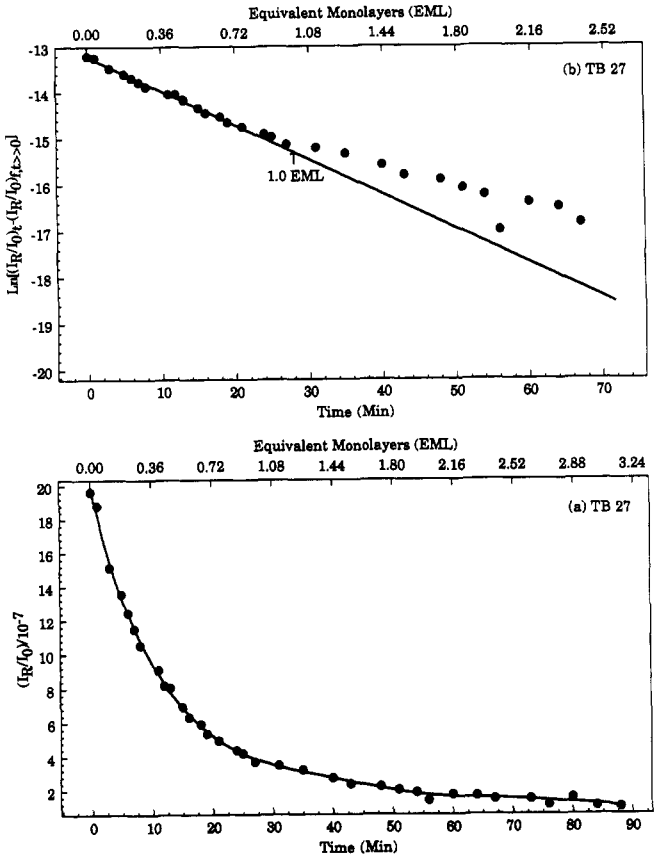

Figure 7. (a) Time (surface coverage, EML CsI) dependence of the intensity of CsI molecules scattered in the specular direction ($\theta_R = 45°$) from NaCl(c,100) for $\theta_I = 45°$. T_{beam}, 726 K; $T_{surface}$, 317 K; flux, 2.7×10^{11} molecules cm^{-2} s^{-1}. (b) Test of a two-state model for condensation of CsI(g) on NaCl(c,100); circles, data from (a); solid line, predicted from the model.

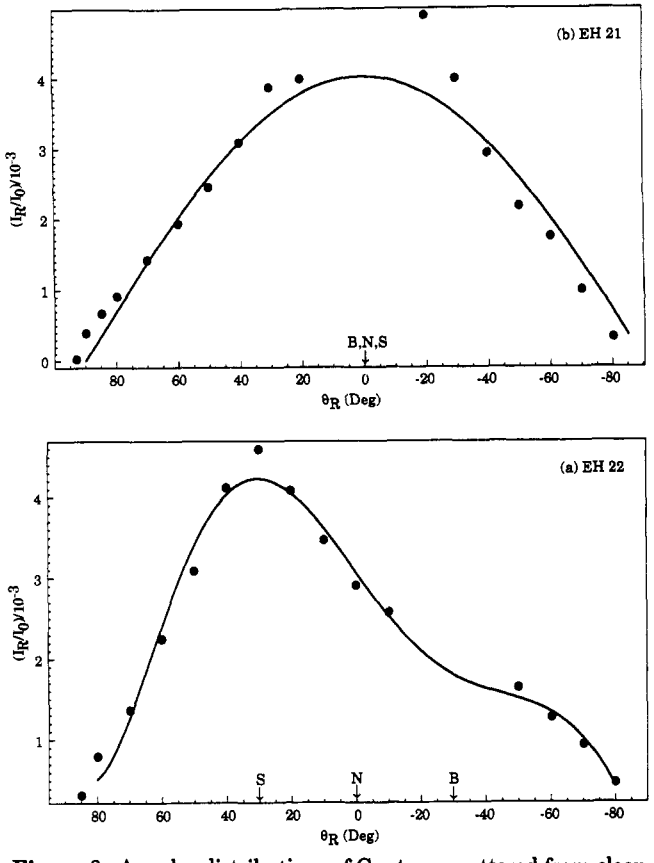

Figure 8. Angular distributions of Cs atoms scattered from clean NaCl(c,100). (a) $\theta_I = 30°$; (b) $\theta_I = 0°$; solid line is best cosine (diffuse component of scattering) fit to data; region between symbols on either side of normal is obscured by the width of the detector.

2. Mechanism of condensation of CsI(g) on NaCl(c,100): The specific form, Figure 7a, of the dependence of I_R on surface coverage suggests a simple two-state model[5] of condensation in which CsI molecules incident on the surface encounter either an occupied or a vacant surface site with different sticking probabilities that are independent of coverage. We obtain excellent agreement between our data, Figure 7a, and predicted behavior, linear dependence of $\ln [(I_R/I_0)_t - (I_R/I_0)_{t,t\gg0}]$ on surface coverage (time, t),[5] Figure 7b, with a two-state model of condensation during an early stage of condensation up to a surface coverage of $\sim^2/_3$ of an equivalent monolayer, at which point deviation of the experimental data from the model commences and becomes larger with increasing coverage of the surface by CsI molecules that condense from the molecular beam. In the early stage of condensation with low surface coverage, the mean distance between CsI molecules on the surface is large and an orienting force between CsI(ads) and the NaCl substrate is dominant. However, as a consequence of poor registry between CsI molecules in the overlayer with ions in the surface of the underlying NaCl(c,100) substrate, lateral CsI–CsI interactions in the adsorbed layer become significant relative to the CsI(ads)/NaCl(c,100) force when crowding of CsI occurs on the surface, at which point the simple two-state model should no longer be adequate to account for condensation of CsI. The two-state model is based on the assumption that there is no appreciable diffusion or large-scale nucleation of CsI on the surface, and in this respect the low coverage results are consistent with calculations[4,8,9] that show that there is a relatively high barrier for diffusion of alkali metal halide molecules on alkali metal halide surfaces. If our model is correct, when lateral interaction of neighboring CsI molecules on the surface becomes important near monolayer coverage, molecular clusters should form nuclei from which small, randomly oriented microcrystals may grow to produce a roughened surface. Hence, on a heavily beam-deposited surface we predict diffuse scattering that is readily apparent in the backscattering region of Figure 5a. From comparison of data in Figures 7, 11, and 12, and Tables I and II, it is clear that structures of both gas and surface play an important role in the condensation processes that we have investigated. However, comparison of experimental results presented here for CsI with those published[5] previously for RbI shows essentially identical behavior for condensation of either alkali metal iodide on both clean and beam-covered NaCl(c,100); a result that together with theoretical calculations[8] of binding energies for CsI(ads)/NaCl(c,100), CsI(ads)/CsI(c), RbI(ads)/NaCl(c,100), and RbI(ads)/RbI(c) suggests that, despite considerably different sizes of CsI and RbI, the factor that dominates condensation behavior in these cases is the large mismatch in registry between the very large ions composing molecules of either the RbI or CsI overlayer and the much smaller ions of the underlying NaCl surface. Of course, best registry with optimum conditions for beam ⇒ surface energy, or momentum, exchange and tight gas–surface binding is

(8) Schoonmaker, R.; Dulles, F.; Mutz, M.; Tucker, T. Extensive unpublished calculations, similar to those described in refs 4 and 9, for several [alkali metal halide(g)/alkali metal halide(c)] systems.

(9) Hove, J. E. *Phys. Rev.* **1955**, *99*, 480.

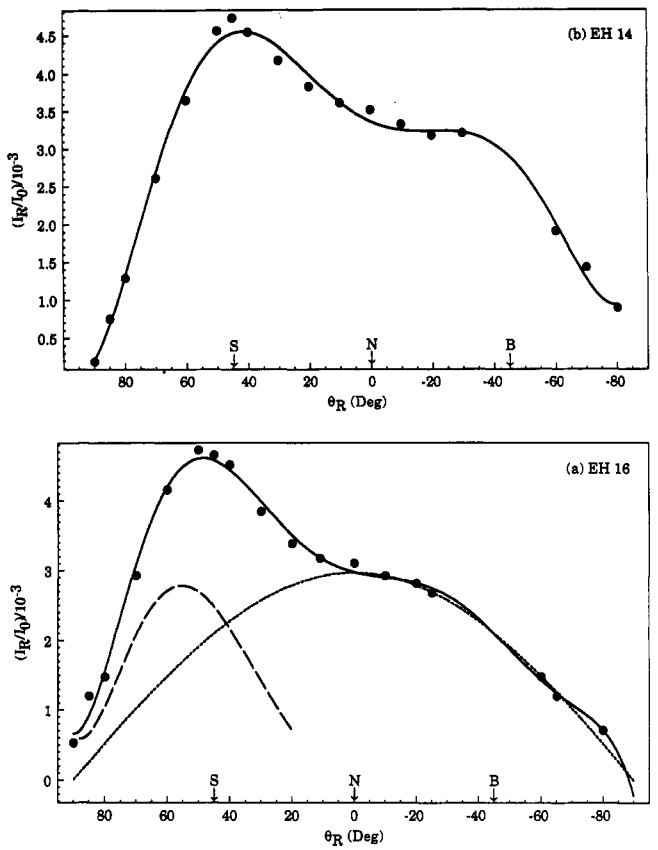

Figure 9. Angular distributions of Cs atoms scattered from NaCl(c,100). (a) $\theta_I = 45°$, clean surface; dotted line is best cosine (diffuse component of scattering) fit in the backscattering region, dashed line is direct-inelastic component of scattering; (b) $\theta_I = 45°$, 1.7 EML of Cs previously deposited on the surface.

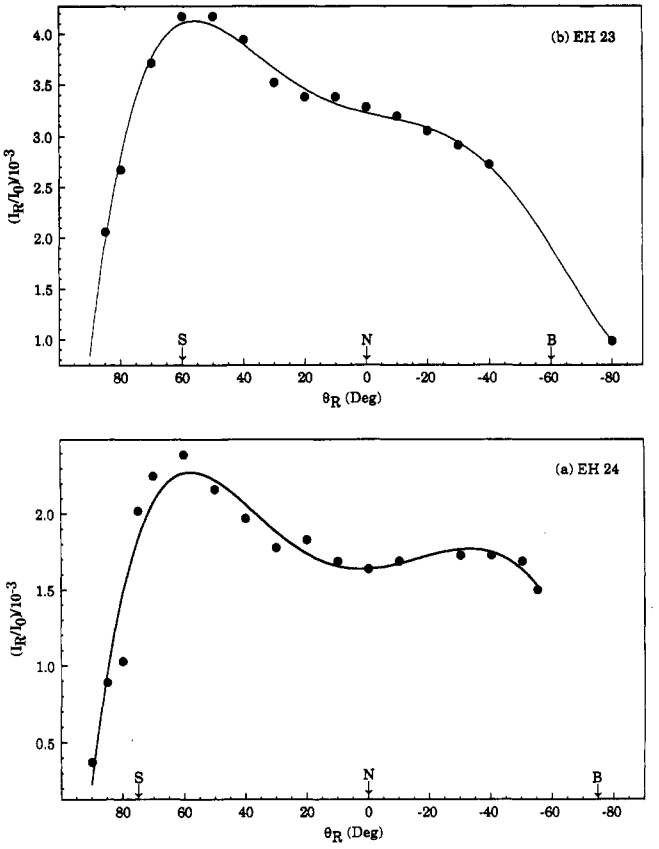

Figure 10. Angular distributions of Cs atoms scattered from clean NaCl(c,100) surfaces. (a) $\theta_I = 75°$; (b) $\theta_I = 60°$.

obtained in those cases where an alkali metal halide gas condenses on its own crystal surface; for example, a heavily alkali metal halide beam-deposited surface.

B. Cs(g)/NaCl(c,100). That there are clear differences in dynamics of gas–surface interactions and mechanisms of condensation is obvious even from cursory perusal of (Figures 8–12) and Table II for Cs atomic beams in comparison with Figures 4–7 and Table I for CsI molecular beams incident on clean and beam-deposited NaCl(c,100).

The angular distribution in Figure 8b was taken with a nominally normal incident atomic beam where scattering should be symmetrical about the normal; however, a small asymmetry is observed that is merely a consequence of θ_I being slightly displaced from 0°. Nevertheless, at, or near, normal incidence, both Cs(g)/NaCl(c,100), Figure 8b, and CsI(g)/NaCl(c,100), Figure 4a, systems exhibit diffuse scattering with a major cosine component and a visible, but mostly obscured, direct-inelastic component, which includes those experimental points between $\theta_R = \pm30°$, and an explanation similar to the one previously given for CsI(g) scattering is applicable to Cs(g) as well. However, unlike CsI(g) beams, Cs(g) beams with $\theta_I \geq 30°$ are scattered from the surface with a large diffuse component that is clearly indicated by the pronounced downward concavity in the backscattering region of angular distributions, Figures 8a, 9, and 10. In this regard, Figure 9a is particularly revealing as it shows that the overall scattering pattern may be decomposed into a small direct-inelastic component and a much larger diffuse component. Cs atoms in the diffuse component of scattering from clean NaCl(c,100) will have had a relatively long lifetime on the surface, because prior to restitution to the gas their perpendicular and parallel components of momentum were

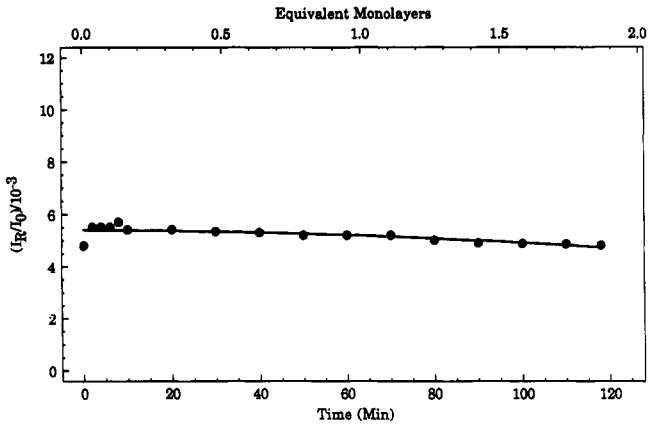

Figure 11. Time (surface coverage, EML Cs) dependence of the intensity of Cs atoms scattered in the specular direction ($\theta_R = 45°$) from NaCl(c,100) for $\theta_I = 45°$. T_{beam}, 679 K; $T_{surface}$, 313 K; flux, 1.3×10^{11} (atoms cm^{-2} s^{-1}).

randomized. Reflection coefficients for Cs, Table II, from clean NaCl(c,100) are approximately 1000 times larger than those for CsI, Table I, which suggests that CsI(ads) is more tightly bound to NaCl(c,100) than is Cs(ads) to NaCl(c,100). The diameter of a Cs atom is 0.530 nm and the lattice spacing of NaCl(c,100) is 0.279 nm, so a single Cs atom may overlap and be polarized by at least part of as many as five ions in the surface of the substrate on which it is adsorbed. Because attraction between a spherically symmetrical Cs(g) atom and substrate ions results only from polarization without regard to orientation, weak binding without directionality is expected—a result that, together with the previously discussed relatively long surface lifetime, suggests that there is little hindrance to diffusion of Cs(ads) on the NaCl surface. Diffusion of Cs atoms on the surface would be consistent with distortion

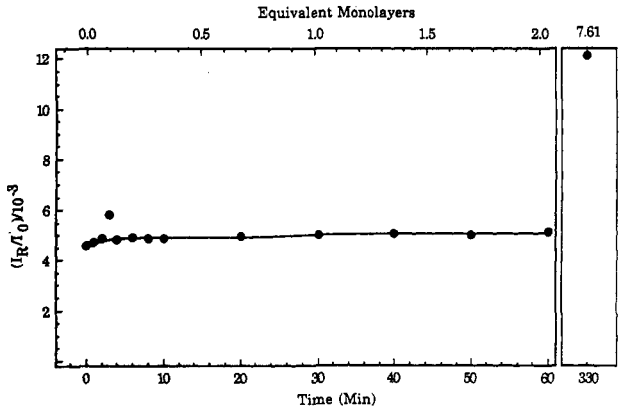

Figure 12. Time (surface coverage, EML Cs) dependence of the intensity of Cs atoms scattered in the specular direction (θ_R = 45°) from NaCl(c,100) for θ_I = 45°. T_{beam}, 739 K; $T_{surface}$, 313 K; flux, 3.1×10^{11} (atoms cm^{-2} s^{-1}). Note break in time (equivalent monolayer) scale.

of cosine, diffuse scattering, components of angular distributions, Figure 10, which may arise near glancing incidence of the atomic beam when randomly directed thermal diffusion on the surface is enhanced in the direction of forward scattering owing to large surface-parallel, forward-directed components of translational energy and momentum of incident gas molecules.

Figures 11 and 12 show that there is no change in the intensity of atoms scattered from the surface at the specular angle over a range of deposition on the NaCl(c,100) surface from 0 to ~2 EML of Cs. Moreover, when beam flux, beam and crystal temperatures, and θ_I remain constant, angular distributions of scattered atoms, Figure 9, and reflection coefficients, Table II, are, within limits of uncertainty in our measurements, indistinguishable for Cs atoms incident on clean NaCl(c,100) and on the same surface after exposure to 1.7 EML of Cs. However, when the surface is exposed to ~7.5 EML of Cs, the intensity of Cs atoms scattered at the specular angle increases by a factor of ~2.5, Figure 12. Thus, when exposed up to ~2 EML of Cs, the NaCl surface appears clean to incident Cs atoms; but when exposed to several additional equivalent monolayers, the NaCl(c,100) surface is altered and it is concluded that in this circumstance Cs atoms in the incident beam strike a surface that is partially, or completely, covered with Cs. We note, also, that changing the Cs flux on the surface by a factor of ~2.5 has negligible affect on the fraction of the incident atomic beam that is reflected, *Figures* 11 and 12, from which we infer that condensation does not occur primarily by multiatom nucleation of Cs in a mobile adsorbed state with subsequent growth of needles, islands, or mountains on the sodium chloride surface.

Now, a crucial question arises: if some of the Cs atoms striking the surface are not scattered back to the gas, but the sodium chloride surface behaves toward the atomic beam as though it were clean over a significant range of equivalent monolayer deposition, what has happened to the Cs atoms incident on the surface that are not scattered back to the gas? The answer is suggested by high mobility of Cs atoms on the surface without nucleation in which case Cs atoms could diffuse across relatively long distances on terraces, where binding energy is relatively small, to ledges and kinks, where binding energy is larger, in the cleaved NaCl(c,100) surface. Cs atoms could then pile up at ledges from which outward growth of Cs eventually would occur. Finally, our results do not rule out the possibility that over a very long period of time some low probability nucleation may occur from which islands of Cs could grow on sodium chloride terraces.

Conclusions

Condensation of gaseous Cs atoms on a sodium chloride surface involves an entirely different mechanism from condensation of gaseous CsI molecules on the same surface.

Gaseous Cs atoms incident on NaCl(c,100) diffuse on the surface over relatively long distances on terraces, and during their mean lifetime in the surface-adsorbed state the atoms either reach kinks and ledges where they stick or are desorbed with an angular distribution that has a large diffuse component characteristic of surface-trapping. In contrast, gaseous CsI molecules incident on NaCl(c,100) either stick at the point of impact with the surface or are restituted to the gas with a direct-inelastic scattering distribution which precludes trapping in a surface-adsorbed state prior to desorption. The different mechanisms of condensation of Cs(g)/NaCl(c,100) and CsI(g)/NaCl(c,100) result from significantly different gas–surface interactions with consequent different dynamics in these two cases.

Acknowledgment is made to the National Science Foundation and to the donors of the Petroleum Research Fund, administered by the American Chemical Society, for support of this research.

Registry No. Cs, 7440-46-2; CsI, 7789-17-5; NaCl, 7647-14-5.